Self-assembly of novel nanowires by thermolysis of fullerene and transition metal thin films

2004 Nanotechnology 15 601

(http://iopscience.iop.org/0957-4484/15/5/034)

INSTITUTE OF PHYSICS PUBLISHING NANOTECHNOLOGY
Nanotechnology **15** (2004) 601–608 PII: S0957-4484(04)73720-4

Self-assembly of novel nanowires by thermolysis of fullerene and transition metal thin films

S Hofmann[1], J Robertson[1], C Ducati[2] and R E Dunin-Borkowski[2]

[1] Department of Engineering, University of Cambridge, Cambridge CB2 1PZ, UK
[2] Department of Materials Science and Metallurgy, University of Cambridge, Cambridge CB2 3QZ, UK

E-mail: sh315@cam.ac.uk

Received 17 December 2003
Published 1 March 2004
Online at stacks.iop.org/Nano/15/601 (DOI: 10.1088/0957-4484/15/5/034)

Abstract
A wide range of nanomaterials has been grown by thermal treatment of patterned condensed-phase precursors. We present a systematic study of the thermolysis of fullerene, amorphous carbon and transition metal thin films, trying to bridge previously reported results in the high temperature regime (>900 °C) and reporting novel structures for low temperature (<550 °C) processing. The synthesis of crystals of single-walled carbon nanotubes from high temperature annealing of patterned, multilayered fullerene and nickel precursor films, could not be reproduced. A thicker fullerene layer in the presence of nickel was, however, transformed into a web-like carbon network. Low temperature processing of similar precursor patterns on sulfur-containing molybdenum grids resulted in the self-assembly of nickel sulfide nanowires and filled MoS_2 nanotubes. Cobalt was found to form cobalt sulfide structures. The strongly oxidizing behaviour of iron resulted in an abundance of needle-like molybdenum oxide crystals. None of the structural formations could be seen for amorphous carbon as a substitutional thin film precursor. Based on the ease of changing precursor materials, this simple, scaleable method addresses many nanomaterials, giving new insight into growth mechanisms as well as offering synthesis control for future applications.

Atomically well-defined one-dimensional nanomaterials could play a key role as building blocks for a future generation of devices as well as provide model systems to demonstrate quantum size effects. Compared to micrometre-diameter structures, nanotubes and nanowires can exhibit remarkable mechanical, electrical and optical properties that are quite different from those of the corresponding bulk materials [1]. Driven by the discovery of new material phases, such as fullerenes [2], considerable progress in the synthesis of such nanostructures has been reported. Arc-discharge, laser-ablation, chemical vapour deposition and solution-based techniques have been developed to synthesize a broad range of nanomaterials [3]. However, only a few methods allow controlled growth directly on a substrate, which is important for many applications, particularly as post-growth manipulation is difficult and expensive in the nanometre size regime.

The annealing of patterned, solid-state precursor materials offers a potentially simple and versatile synthesis route with excellent positional control. The cheap and flexible use and change of precursors make it attractive for studying the growth of many different nanostructures. Unlike other techniques, the process relies only on widespread, standard thin film equipment, and does not require expensive growth chambers and maintenance. It allows selective synthesis on a substrate and is scaleable for applications.

Several condensed-phase annealing experiments have been reported [4–6], most prominently the alleged self-assembly of single crystals of single-walled carbon nanotubes from nanopatterned structures of alternating layers of C_{60} and nickel [7, 8]. Similar to other techniques such as chemical vapour deposition [9], in these experiments the transition metal is supposed to act as a catalyst, effectively converting the

precursor into a new nanostructure. However, despite using similar precursors and processing conditions, the results of individual studies vary widely [4, 7, 10, 11], suggesting the need for a more detailed, comparative study.

This paper presents a systematic study of the thermolysis of C_{60}/C_{70}, amorphous carbon (a-C) and transition metal thin films, trying to bridge previously reported results in the high temperature regime (>900 °C) and reporting novel structures in the low temperature regime (<550 °C). We could not reproduce the synthesis of crystals of single-walled carbon nanotubes by this method, as reported earlier [10]. Instead, molybdenum oxide compounds were found to form from the substrate material, rather than from the thin film precursors [8, 10, 11]. We find, however, that a thicker fullerene layer can be converted into a buried graphitic network [4, 5]. Because high processing temperatures restrict the choice of substrate material and integration processes, we focus on low temperature processing and the influence of the carbon and metal films in the precursor pattern. For a thin fullerene layer, the metal forms long compound nanowires, rather than being a passive catalyst. At temperatures below 550 °C, Ni self-assembles into high-aspect ratio sulfide crystals [10]. We widened the study to include Co, Fe and a-C as precursor materials, and report here a detailed electron microscopy study of the as-grown structures as a function of precursor stacking, annealing atmosphere and temperature.

1. Experimental details

The approach that we use is based on the annealing of patterned thin film precursor materials in a controlled atmosphere. Pillars of alternating fullerene and metal layers were formed by evaporating C_{60}/C_{70} powder (fullerite, Sigma-Aldrich) and high purity metal wire from tungsten boats mounted on a four turret source in a standard evaporator. The use of four evaporation sources gives a large variety of possible layer-by-layer precursor structures. The fullerite powder was degassed for several minutes before sublimation. The system was allowed to return to its base pressure of 10^{-6} mbar after the deposition of each individual layer. Unless otherwise stated, the films were condensed onto sulfur-containing 300 mesh Mo TEM grids (Agar Scientific). The use of TEM grids as substrate material makes the as-grown nanostructures readily accessible for subsequent TEM analysis in their original growth environment, rather than having to disperse and transfer them. In contrast to most commercially available grids, Mo TEM grids are etched and not electroplated, which makes them suitable for high temperature annealing experiments. However, as a result of adsorption at the metal surface during wet etching, sulfur is a major contaminant of Mo grids, which is a crucial factor when considering higher, temperature-activated diffusivities.

As a substitute for the fullerene material, amorphous carbon layers were grown from acetylene by plasma enhanced chemical vapour deposition in a parallel plate configuration. The conditions (100 W radio-frequency (RF) power, 200 mTorr C_2H_2) were chosen to give a predominantly sp^2-bonded, more reactive amorphous network. Sandwich structures of up to nine alternating layers of a-C and Ni were deposited. In this case, the vacuum had to be broken to transfer the samples for successive layers. The thicknesses of the individual a-C layers were similar to those of the fullerene films.

Patterning on uneven substrates was achieved by using Cu TEM grids as disposable shadow masks, the highest mesh (2000) leading to a 10 μm × 10 μm feature size with a 10 μm pitch. The patterning dimensions and the thicknesses of the individual layers were measured by atomic force microscopy (AFM, Digital Instruments Nanoscope III).

The as-prepared samples were transferred to a vacuum system fitted with a ceramic heating element (Elstein–Werk). After evacuation to below 10^{-6} mbar, the chamber was refilled with nitrogen (5.0 grade). Samples were typically processed at 5–10 mbar and 510–550 °C for up to 1 h. Alternatively, pre-patterned samples were annealed in high temperature furnaces at 950 °C, either in vacuum (base pressure 10^{-6} mbar) or in an inert gas flow for times varying from a few minutes to an hour. The structures and compositions of the nanocrystals were analysed by a combination of scanning electron microscopy (SEM, Jeol 6340 FEGSEM), high-resolution transmission electron microscopy (HREM, Jeol JEM 4000EX, 400 kV), energy dispersive x-ray spectroscopy (EDX), electron energy loss spectroscopy (EELS, Philips CM300ST, 300 kV and VG HB501 STEM, 100 kV) and Raman spectroscopy (Renishaw RM series).

2. Results and discussion

Figure 1(a) shows an SEM image of a Mo TEM grid patterned with multilayered pillars of sublimed C_{60}/C_{70}–Ni layers. The individual pillars are roughly 150 nm in height (figure 1(b)), consisting of typically nine C_{60}/C_{70} and Ni layers with individual thicknesses varying from 40 to 2 nm. The pillars were initially designed to repeat the reported synthesis of single crystals of single-walled carbon nanotubes catalytically self-assembled from the fullerene precursors [7]. The patterned grids were heated to 950 °C in vacuum as in the original publication. Nanorods emerged perpendicular to the surface, even in the absence of an external magnetic field. However, the structures do not correlate with the precursor stacks. Rather than originating from the patterned multilayers, the nanorods are found in unpatterned, precursor-free regions of the Mo TEM grid (figure 2(a)), as well as on annealed empty Mo TEM grids. The nanorods are up to 1 μm long and typically 100 nm in diameter. HREM analysis revealed a high degree of crystallinity (figure 2(b)). Longitudinal fringes with a spacing of 3.83 Å parallel to the long axis are observed, similar to the original report [7]. This spacing corresponds to that of MoO_3 (011) planes (see inset figure 2(b)), as confirmed by EELS elemental mapping, which showed that the crystals are molybdenum oxide structures. Following our initial observation [10], several other groups [11] also independently concluded that the single crystals reported by Schlittler *et al* [7, 12] were not composed of single-walled carbon nanotubes, but were molybdenum oxide structures. Schlittler *et al* [7] reported the same structures on silicon dioxide substrates, which could also not be reproduced and are equally questionable considering the crystals originating from the Mo substrates.

However, previous work reports the synthesis of carbon structures from similar precursors and conditions [4]. High

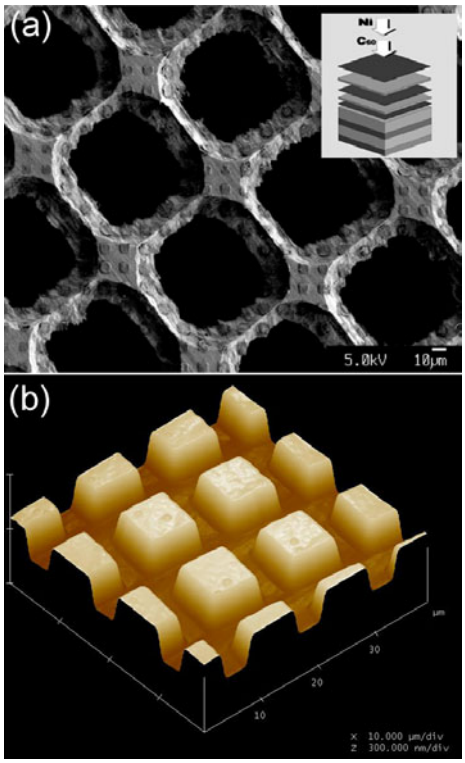

Figure 1. (a) SEM photograph of a 300 mesh Mo TEM grid with multilayered pillars of sublimed C_{60}/C_{70} and Ni. The inset shows a schematic of the deposition process. (b) Atomic force microscopy (AFM) image of patterned precursor pillars.

(This figure is in colour only in the electronic version)

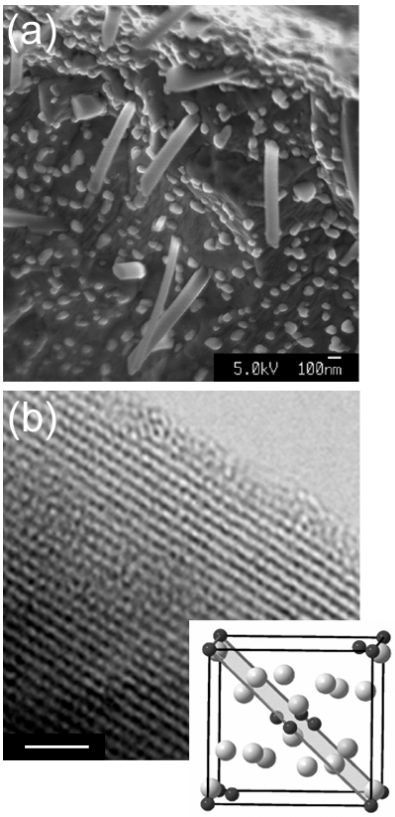

Figure 2. C_{60}/C_{70}–Ni multilayer on a Mo TEM grid processed at 950 °C in vacuum for 1 h: (a) SEM photograph of region between precursor pillars, (b) bright-field HREM image of observed nanocrystals (scale bar 2 nm). The inset shows a computer model of a MoO_3 monoclinic cell where molybdenum and oxygen atoms are represented in dark and light grey, respectively. The plane identified within the cell is a $MoO_3(011)$ plane (spacing 3.83 Å).

temperature annealing of alternating films of C_{60} and Ni patterned on silica resulted in the formation of graphitic Ni-filled carbon nanotubes [4]. By using thicker fullerene layers (>40 nm) in the precursor stacking, we observed a web-like carbon network after vacuum annealing at 950 °C (figure 3(a)). The individual structures are typically 15 nm in diameter and strongly entangled. Compared to the MoO_3 crystals, the carbon structures are not free-standing, but buried in the precursor pillar and are only exposed through cracks in the covering layers. HREM analysis shows a rather low degree of graphitization (figure 3(b)). The result shows, however, that the fullerene layer can act as a carbon precursor.

In addition to fullerenes, amorphous carbon has been reported to act as a solid-phase precursor for the formation of multi-walled carbon nanotubes [13]. Diamond-like carbon flakes mixed with Ni were transformed by annealing at 1200 °C for 3 h [13]. In analogy to the fullerene patterns, we deposited a-C and Ni multilayers on free-standing silicon nitride membranes (figure 4(a)). This approach gives good precursor mixing based on the multilayer stacking. In addition, the as-grown structures can be patterned and analysed through the electron-beam transparent membrane. Instead of predominantly sp^3-bonded diamond-like carbon, we used less inert, mainly sp^2 bonded, hydrogenated a-C. Annealing at 950 °C in nitrogen for 1 h did not, however, result in the formation of any high aspect ratio structures on the surface (figure 4(b)). Instead, the pillars appear to dissolve into spherical nanostructures, most likely Ni islands covered in a-C. Thin Ni films are known to break up into small islands upon annealing due to surface tension and compressive stress [9]. Compared to fullerene layers, the a-C films give a more rigid structure of the initial precursor stacks, allowing less mixing during the annealing process.

At present, a disadvantage of condensed-phase precursor methods is the high annealing temperature, restricting the choice of substrate materials and integration processes. Rather than processing in high-temperature furnaces, we therefore also processed the patterned precursor arrays in a vacuum system fitted with a comparatively small area (20 cm^2) custom built ceramic heating element. Figure 5 shows SEM images of a patterned 300 mesh Mo TEM grid processed at 530 °C in 5 mbar nitrogen for 30 min. Self-assembled nanostructures originate from the heavily reacted precursor pillars at the top (figure 5(a)), as well as at the edge (figure 5(b)) of the grid, being readily accessible for TEM analysis. The rod-shaped structures are less than 100 nm in diameter and more than 10 μm in length. No such structures are seen between the pillars, demonstrating the possible selective positioning. HREM revealed that the as-grown nanowires are highly crystalline (figures 6–8). Although no sulfur had been introduced deliberately during the patterning and synthesis process, the nanowires were identified as $Ni_xS_yC_z$ compounds from EDX and EELS analysis. This indicates the sensitivity of the method to impurities, the sulfur originating

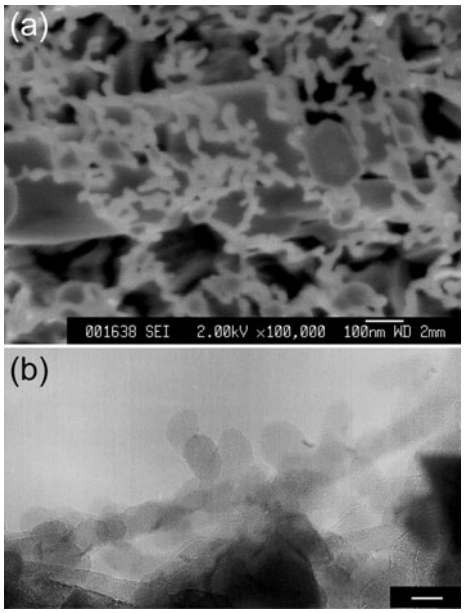

Figure 3. Thick C_{60}/C_{70} layers on a Mo substrate sandwiched between Ni films processed at 950 °C in vacuum for 1 h: (a) SEM photograph of the precursor pillar, (b) bright-field HREM image of the observed carbon structures (scale bar 15 nm).

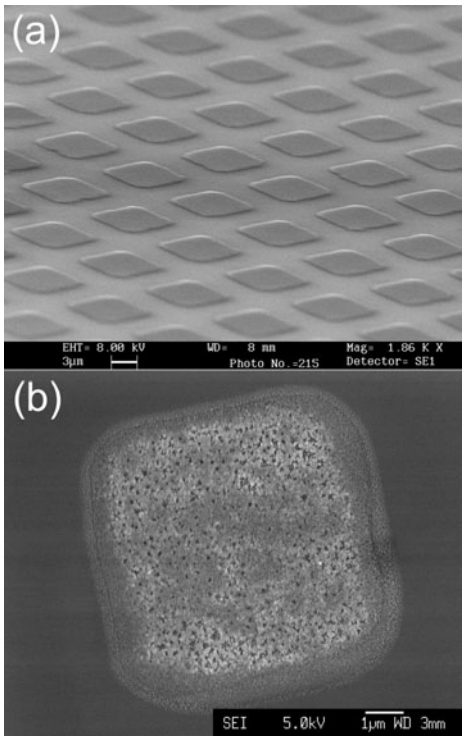

Figure 4. a-C/Ni multilayer on a silicon nitride membrane processed at 950 °C in nitrogen for 1 h: (a) SEM photograph of an unannealed patterned membrane, (b) SEM photograph of an annealed individual multilayer stack.

from contamination of the Mo substrates. Figure 6(a) shows two crystalline nanowires of about 19 and 12 nm diameter. In figure 6(b), a magnified portion of the wider structure shows lattice fringes of 2.97 Å parallel to the wire axis. We identified the fringes as the (300) planes of a $Ni_{17}S_{18}$ trigonal

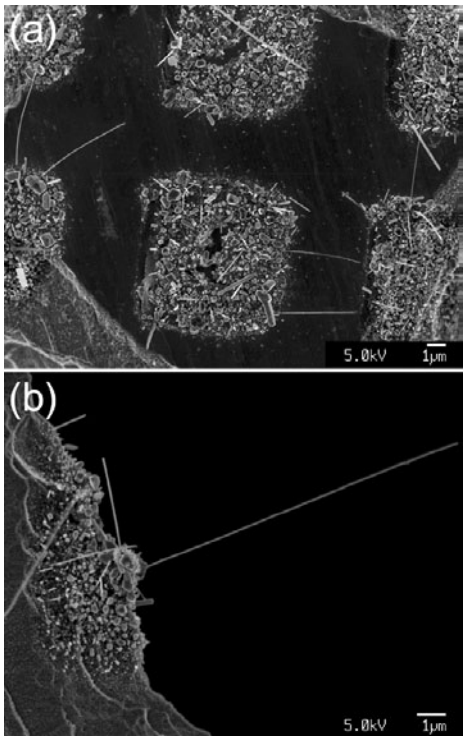

Figure 5. SEM photographs of self-assembled structures originating from multilayered C_{60}/C_{70} and Ni pillars at the (a) top, and (b) edge of a 300 mesh Mo TEM grid processed at 530 °C in 5 mbar N_2 for 30 min.

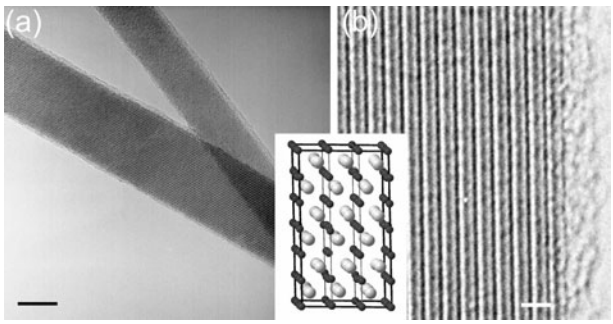

Figure 6. (a) Crystalline Ni sulfide nanowires 19 and 12 nm in diameter, (b) magnified portion of the wider structure showing 2.97 Å lattice fringes parallel to the wire axis. The inset shows a computer model of a $Ni_{17}S_{18}$ trigonal cell where nickel and sulfur atoms are represented in dark and light grey, respectively. The {300} planes are identified within the cell (spacing: 2.97 Å) (scale bars: (a) 10 nm, (b) 1 nm).

cell, represented in the inset using a ball-and-stick computer model. To enhance visualization, the (300) planes are marked with vertical lines within the cell. Carbon was found along the nanowire and its amorphous surface layer, indicating that fullerenes may act as a carbon source even at comparatively low temperatures. The nanocrystals were observed to be stable in the electron beam and did not suffer irradiation damage.

Analysing nanostructures on processed-patterned, sulfur-contaminated Mo grids by HREM, we found not only high aspect ratio sulfide nanocrystals but also layers of MoS_2 surrounding these structures. Figure 7 shows such heterostructures synthesized at 550 °C in 10 mbar nitrogen in 1 h. Figure 8(a) shows a magnified portion of the MoS_2

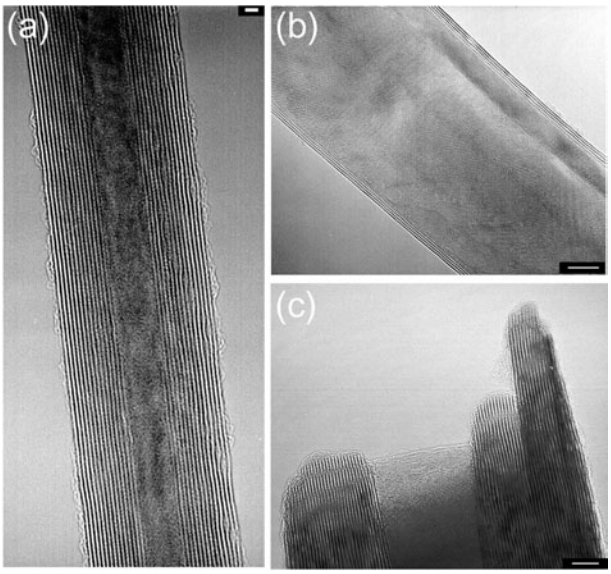

Figure 7. HREM images of MoS_2 layers surrounding high aspect ratio Ni sulfide structures (scale bars: (a) 2 nm, (b) and (c) 5 nm).

compound structure shown in figure 7(a). A set of 14 outer walls parallel to the wire axis with a characteristic spacing of 6.2 Å can be seen. The lattice fringes in the core correspond to the 3.10, 2.85 and 2.75 Å spacings of $Ni_{17}S_{18}$. EEL spectra acquired at the periphery as well as at the central part of the wire confirm its composite nature (figure 8(b)). Carbon is found both in the outer walls and in the core of the wire, and some amorphous carbon was observed surrounding the nanocrystal. It is reasonable to assume that C atoms form a misfit compound within the MoS_2 layered structure, and that they occupy substitutional sites in the $Ni_{17}S_{18}$ lattice. Raman spectra of the filled MoS_2 structures closely resemble the previously published signals of platelet MoS_2 samples [14].

The growth process was studied further by using different stacking orders within the pillars of the precursor materials, starting with substrates carrying solely one precursor. Under identical low temperature processing conditions, neither pure patterned Ni nor C_{60}/C_{70} alone, when sublimed through a 2000 mesh Cu grid, led to any high aspect ratio sulfide crystals. In contrast, one Ni layer sandwiched between two C_{60}/C_{70} layers yielded long nanowires similar to the multi-layered precursor structure described above. It is interesting to note that processing pure fullerene pillars leaves hardly any material on the pattern, suggesting that Ni acts as a sublimation barrier.

Analogous to the high temperature processing (figure 4), the fullerene material was substituted by a-C layers. The multilayered a-C/Ni stacks were patterned on Mo TEM grids and processed at 540 °C in 10 mbar nitrogen for 1 h. In contrast to the C_{60}/C_{70} layers (figure 5), no sulfide nanowires could be grown. From these experiments, we infer that the fullerene layer plays an active role in the synthesis, providing a high surface area, low density environment in which the diffusion and mixing of the constituent elements can take place [15].

Transition metals other than Ni were included in the precursor pillar, maintaining the multilayer stacking and individual layer thicknesses. Figure 9 shows a C_{60}/C_{70} and Co patterned 300 mesh Mo TEM grid processed at 550 °C in 10 mbar nitrogen for 1 h. Compared to Ni (figure 5), significantly fewer nanostructures self-assemble out of the Co containing pillars (figure 9(a)). The structures resemble the Ni sulfide wires in shape and dimensions (figure 9(b)). HREM analysis shows that the structures are highly crystalline (figure 9(c)). The nanowires were identified as Co sulfide compounds by EDX and EELS analysis (figure 10). Figure 10(b) shows the characteristic sulfur and cobalt ionization edges in the EEL spectrum. In some cases, carbon could also be detected in the structures. The crystals (figure 10(a)) were found to be stable and did not exhibit any beam damage. This indicates the versatility of the method: by including different elements in the precursor pillars, a large variety of new materials might be synthesized. No MoS_2 layers were found surrounding the Co containing crystals.

Figure 11 shows C_{60}/C_{70} and Fe pillars on a 300 mesh Mo TEM grid processed at 550 °C in 10 mbar nitrogen for 1 h. Unlike the Ni and Co patterning, the processed fullerene/Fe pillars extend into the unpatterned substrate (figure 11(a)), being surrounded by a halo of grainy material with emerging needle-like structures (figure 11(b)). The structures are typically 5 nm in diameter and not longer than 200 nm. HREM analysis shows the core of these needle-like structures to be highly crystalline, surrounded by an amorphous outer layer (figure 11(c)). Figure 12 shows the results of EELS elemental mapping of a single needle-like structure and the surrounding material. Three-window background-subtracted elemental maps were acquired using the molybdenum M edge (227 eV), the oxygen K edge (532 eV) and the iron L edge (708 eV) on a 2048 × 2048 pixel charge-coupled-device (CCD) camera. The chemical maps represent the projected elemental concentrations in the electron beam direction. The maps show that, despite the surrounding base region being mainly iron oxide, the structure itself is a molybdenum oxide crystal, in which no Fe is incorporated. Figure 12(c) shows an individual EEL spectrum of the structure, exhibiting solely the characteristic Mo and O ionization edges. No clear signature of sulfur could be detected. As for high temperature annealing of fullerene/Ni patterns (figure 2), the Mo originates from the substrate grid. With Fe, however, the Mo oxide structures show a correlation to the patterned precursor stacks. The strongly oxidizing behaviour of Fe appears to enhance the formation of Mo oxide structures, resulting in an abundance of those needle-like structures in the vicinity of the original fullerene/Fe pillars. Also for the low temperature annealing of Ni and Co containing precursors, very small Mo oxide crystals could sometimes be seen. However, their randomly scattered appearance can be clearly distinguished from the comparatively long sulfide crystals correlated directly to the precursor pillars.

Nickel, cobalt and iron sulfides have been the subject of considerable interest, primarily because of their potential catalytic applications in hydrodenitrogenation [16] and hydrodesulfurization processes, in particular the removal of sulfur and sulfur containing compounds from gas and oil [17]. Typically, these sulfides are prepared by solid-state and vapour-phase reactions [18, 19], but solution based techniques have also been reported [20, 21]. Rodriguez *et al* [22] reported the formation of bulk nickel and iron sulfide from the low temperature annealing of transition metal films on S/Mo structures. This study shows that both Ni and Fe can promote Mo/S interactions, and the subsequent formation of

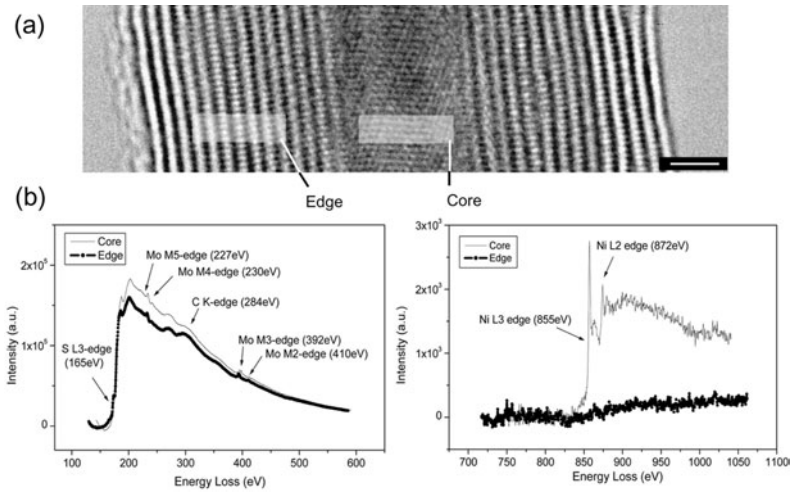

Figure 8. (a) Magnified portion of the MoS_2 compound structure shown in figure 7(a). A set of 14 outer walls parallel to the wire axis with a characteristic spacing of 6.2 Å can be seen. The lattice fringes in the core correspond to the 3.10, 2.85 and 2.75 Å spacings of $Ni_{17}S_{18}$. Carbon is found both in the outer walls and in the core of the wire (scale bar 2 nm). (b) Corresponding EEL spectra of the edge and core region of the structure, showing the region of S, C and Mo ionization edges (left), and the Ni ionization edges (right). The absence of an Ni peak from the spectrum acquired at the outer walls confirms the heterogeneous character of the nanowire.

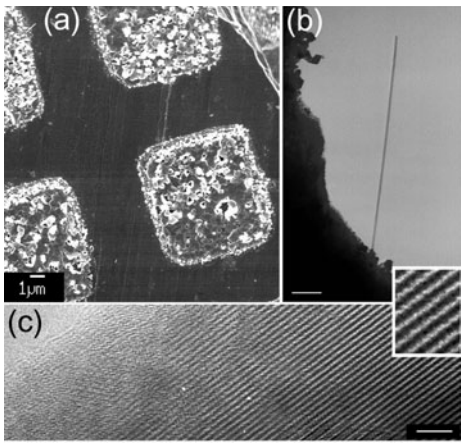

Figure 9. (a) SEM photograph of multilayered C_{60}/C_{70} and Co pillars on top of a 300 mesh Mo TEM grid processed at 550 °C in 10 mbar N_2 for 1 h. (b) TEM image of a self-assembled structure originating from a C_{60}/C_{70} and Co stack at the edge of a grid (scale bar 500 nm). (c) HREM image of a portion of a Co sulfide nanowire. The inset shows magnified lattice details (scale bar 3 nm).

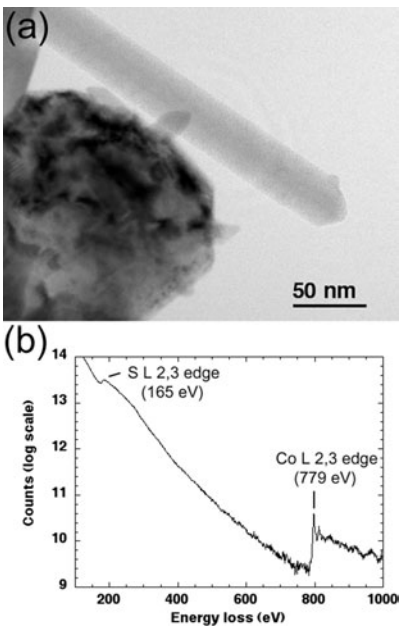

Figure 10. EELS measurement of self-assembled crystals from C_{60}/C_{70} and Co pillars. The bright field image was acquired slightly under focus (a). The EEL spectrum shows the Co and S ionization edges (b).

molybdenum sulfides. The promotional effect is much larger for Ni than for Fe [22]. Focusing on the low temperature processing of our precursor stacks on sulfur contaminated Mo grids, this might help to understand the formation of Ni and Co sulfide compounds and, in the case of Ni, even the formation of surrounding MoS_2 layers. However, in the present study the annealing of a single Ni layer on the contaminated Mo grids did not lead to any high aspect ratio sulfide crystals, neither did the processing of multilayered a-C/Ni stacks. The fullerene layers, therefore, play an active role in the synthesis, at least in providing a high surface area reactive environment. Transition metal sulfides can exist in many phases. The synthesis of a specific phase critically depends on the synthesis conditions, such as temperature [18]. This may explain the differences between the use of Ni and Co precursors and the absence of sulfides when using high temperature furnace processing.

The argument above cannot, however, account for the intriguing high aspect ratio crystal geometry of the as-grown sulfides (e.g. figure 5). Solution based techniques showed the formation of one-dimensional Ni sulfide structures [20, 21]. Layer-rolled NiS structures are thought to form based on the crystal structure of the hexagonal NiS phase [20]. The growth mechanism for solid NiS and Ni_9S_8 nanorods is speculated to be a molecular-template-like process based on the coordination ability of various complexes in solution [21]. Growth models for metal dichalcogenide nanostructures typically suggest a conversion process starting from an oxide template, whereby

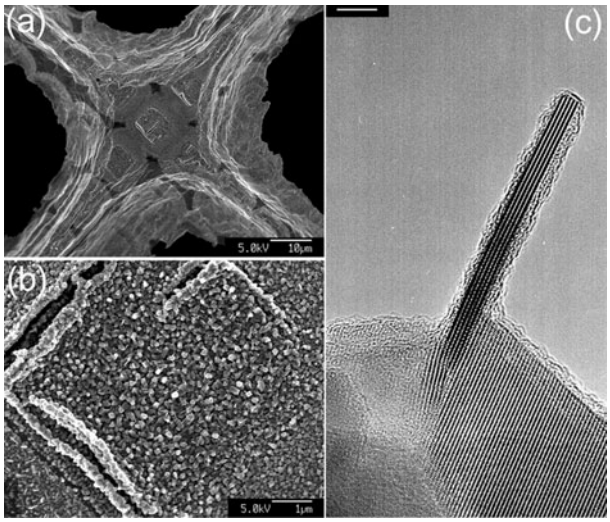

Figure 11. (a) SEM photograph of multilayered C_{60}/C_{70} and Fe pillars on top of a 300 mesh Mo TEM grid processed at 550 °C in 10 mbar N_2 for 1 h. (b) Close-up of (a), showing a single multistack. (c) HREM of structures at the edge of the Mo grid (scale bar 5 nm).

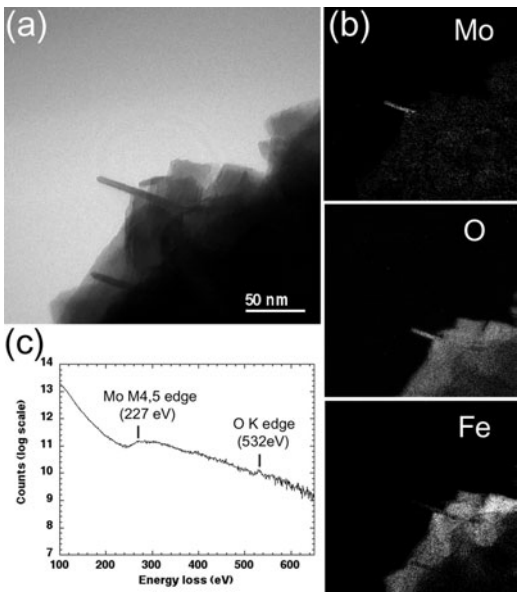

Figure 12. EELS elemental mapping of structures at the edge of a C_{60}/C_{70} and Fe patterned Mo grid. (a) Bright field image, showing a single needle-like structure and its surroundings. (b) Three-window background-subtracted elemental maps were acquired using the molybdenum M edge (227 eV), the oxygen K edge (532 eV) and the iron L edge (708 eV) on a 2048 × 2048 pixel CCD camera (the Fe signal of the needle-like structure only contains noise, no Fe was detected in the structure; scales are identical to (a)). (c) An individual EEL spectrum of the structure, showing Mo and O ionization edges.

the sulfur slowly replaces the oxygen [23]. This conversion model would predict a residual oxide core inside, for instance, a MoS_2 nanotube. Recently a 'nuclei-radiation' growth model for the formation of Mo_2S_3 nanorods was proposed [24]. Rather than acting as a template, the MoO_3 is thought to serve as a nucleus for the radiant growth of sulfide nanorods without oxide inclusion. The small molybdenum crystals found on our TEM grids could, under suitable conditions, act as nuclei for high aspect ratio sulfide crystals.

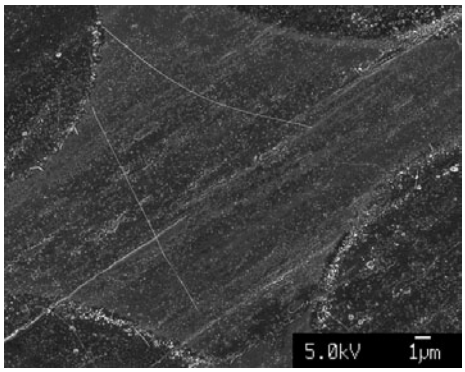

Figure 13. SEM photograph of self-assembled nanostructures originating from multilayered C_{60}/C_{70}–Ni patterns on a Mo sheet processed at 510 °C in 5 mbar nitrogen for 30 min. The modified precursor pillars only allow lateral growth originating from the pillar edge.

Technologically, any potential synthesis method for future applications involving the integration of nanostructures requires the ability to select growth position and orientation. Figure 13 shows self-assembled nanostructures originating from multi-layered C_{60}/C_{70}–Ni patterns on a Mo sheet processed at 510 °C in 5 mbar nitrogen for 30 min. By covering the top of the precursor pillar with a thick Ni layer (or an other suitable metal), the nanowires now emerge from the side of the pillar, showing the potential of selective lateral growth using this simple method. An additional electric field could be applied between the precursor stacks, potentially aligning the self-assembling structures. In order to achieve a more controlled supply of Mo and S, we are currently working on including both elements in the precursor stacking to be sublimed on Si substrates. This could be achieved, for instance, by including fullerene-like MoS_2 nanoparticles [25] in the pillars, or by annealing Mo containing pillars in H_2S.

3. Conclusions

In conclusion, a systematic study of the thermolysis of fullerene, amorphous carbon and transition metal thin films on sulfur containing Mo substrates has been presented. The reported synthesis of crystals of single-walled carbon nanotubes from fullerene and nickel precursor films could not be reproduced. A thick fullerene layer in the presence of nickel was, however, seen to give a web-like carbon network upon high temperature annealing. Low temperature processing of similar precursor patterns in an inert atmosphere resulted in the self-assembly of nickel sulfide nanowires and compound-filled MoS_2 nanotubes. Cobalt, when used as a substitutional transition metal in the precursor stack, could also be incorporated into self-assembled cobalt sulfide structures, indicating the versatility of the method. Rather than forming sulfide structures, the strongly oxidizing behaviour of iron resulted in the growth of needle-like oxide crystals. The special role of the fullerenes in the growth process is emphasized by the fact that none of the structural formations can be seen for amorphous carbon as a substitutional thin film carbon precursor. The low temperature synthesis route for sulfide structures offers selective positioning and alignment, being potentially interesting for device integration. Based on the ease

of changing precursor materials, this simple, scaleable method could be used to synthesize a wide range of nanomaterials, giving new insight into growth mechanisms and offering synthesis control for future applications.

Acknowledgments

This work was supported by the European Union (CARBEN). The authors thank A C Ferrari and D P Chu for Raman and AFM measurements, respectively. The help of F Piazza with the a-C thin film depositions is acknowledged. REDB acknowledges the Royal Society and the EPSRC for financial support.

References

[1] Alivisatos A P 1996 *Science* **271** 933
[2] Kroto H W, Heath J R, O'Brien S C, Curl R F and Smalley R E 1985 *Nature* **318** 162
[3] Xia Y N, Yang P D, Sun Y G, Wu Y Y, Mayers B, Gates B, Yin Y D, Kim F and Yan Y Q 2003 *Adv. Mater.* **15** 353
[4] Grobert N, Terrones M, Osborne A J, Terrones H, Hsu W K, Trasobares S, Zhu Y Q, Hare J P, Kroto H W and Walton D R M 1998 *Appl. Phys.* A **67** 595
[5] Kanzow H, Ding A, Nissen J, Sauer H, Belz T and Schlogl R 2000 *Phys. Chem. Chem. Phys.* **2** 2765
[6] Doherty S P and Chang R P H 2002 *Appl. Phys. Lett.* **81** 2466
[7] Schlittler R R, Seo J W, Gimzewski J K, Durkan C, Saifullah M S M and Welland M E 2001 *Science* **292** 1136
[8] Welland M E, Durkan C, Saifullah M S M, Seo J W, Schlittler R R and Gimzewski J K 2003 *Science* **300** 1236
[9] Hofmann S, Ducati C, Robertson J and Kleinsorge B 2003 *Appl. Phys. Lett.* **83** 135
[10] Hofmann S, Ducati C and Robertson J 2002 *Adv. Mater.* **14** 1821
[11] Chisholm M F, Wang Y H, Lupini A R, Eres G, Puretzky A A, Brinson B, Melechko A V, Geohegan D B, Cui H T, Johnson M P, Pennycook S J, Lowndes D H, Arepalli S, Kittrell C, Sivaram S, Kim M, Lavin G, Kono J, Hauge R and Smalley R E 2003 *Science* **300** 1236
[12] Moore S K 2002 *IEEE Spectr.* **39** 22
[13] Sarangi D, Godon C, Granier A, Moalic R, Goullet A, Turban G and Chauvet O 2001 *Appl. Phys.* A **73** 765
[14] Frey G L, Tenne R, Matthews M J, Dresselhaus M S and Dresselhaus G 1999 *Phys. Rev.* B **60** 2883
[15] Coq B, Planeix J M and Brotons V 1998 *Appl. Catal.* A **173** 175
[16] Cid R, Atanasova P, Cordero R L, Palacios J M and Agudo A L 1999 *J. Catal.* **182** 328
[17] Welters W J J, Vorbeck G, Zandbergen H W, Dehaan J W, Debeer V H J and Vansanten R A 1994 *J. Catal.* **150** 155
[18] Tilley R D and Jefferson D A 2002 *J. Phys. Chem.* B **106** 10895
[19] Lauritsen J V, Helveg S, Laegsgaard E, Stensgaard I, Clausen B S, Topsoe H and Besenbacher E 2001 *J. Catal.* **197** 1
[20] Jiang X C, Xie Y, Lu J, Zhu L Y, He W and Qian Y T 2001 *Adv. Mater.* **13** 1278
[21] Shen G Z, Chen D, Tang K B, An C H, Yang Q and Qian Y T 2003 *J. Solid State Chem.* **173** 227
[22] Rodriguez J A, Li S Y, Hrbek J, Huang H H and Xu G Q 1997 *Surf. Sci.* **370** 85
[23] Feldman Y, Frey G L, Homyonfer M, Lyakhovitskaya V, Margulis L, Cohen H, Hodes G, Hutchison J L and Tenne R 1996 *J. Am. Chem. Soc.* **118** 5362
[24] Che R C, Bai N and Peng L M 2003 *Appl. Phys. Lett.* **83** 3561
[25] Feldman Y, Wasserman E, Srolovitz D J and Tenne R 1995 *Science* **267** 222